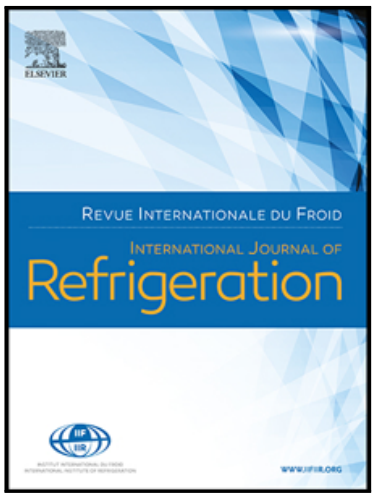

Evaluating the performance of a coated tube adsorber for adsorption cooling

João M.S. Dias , Vítor A.F. Costa

PII: S0140-7007(20)30278-4
DOI: https://doi.org/10.1016/j.ijrefrig.2020.06.023
Reference: JIJR 4819

To appear in: *International Journal of Refrigeration*

Received date: 9 March 2020
Revised date: 16 June 2020
Accepted date: 19 June 2020

Please cite this article as: João M.S. Dias , Vítor A.F. Costa , Evaluating the performance of a coated tube adsorber for adsorption cooling, *International Journal of Refrigeration* (2020), doi: https://doi.org/10.1016/j.ijrefrig.2020.06.023

Highlights

- A well-established model used for the dynamic simulation of a coated tube adsorber.
- Performance evaluation of a coated tube adsorber for cooling applications.
- Influence of several governing parameters on the adsorber's performance.
- Optimization of the key parameters for adsorption cooling.

Evaluating the performance of a coated tube adsorber for adsorption cooling

João M.S. Dias [a,*], Vítor A.F. Costa [a]

[a] TEMA – Centre for Mechanical Technology and Automation, Department of Mechanical Engineering, University of Aveiro, Campus Universitário de Santiago, 3810-193 Aveiro, Portugal

*** Correspondence:**
João M.S. Dias
Tel: +351 234 370 830
Email: joaomdias@ua.pt
web: Research ID, ORCID, http://www.ua.pt

Abstract

Adsorption cooling (AC) is an environmentally friendly alternative to conventional vapor compression cooling. In this paper, the performance of a coated tube adsorber suitable for AC systems is numerically evaluated. The developed adsorber uses silica gel-water as adsorbent-adsorbate working pair. A numerical model is used to analyze the influence of several governing parameters such as the evaporator, condenser and regeneration temperatures, cycle time, metal-adsorbent heat transfer coefficient, metal tube diameter, coating thickness and heat transfer fluid (HTF) velocity on the adsorber's performance. It is confirmed that increasing the evaporator temperature results on a performance increase whereas increasing the condenser temperature hindrances the system's performance. A regeneration temperature close to 70 ^{o}C results on the highest cooling coefficient of performance (COP_c). The cycle time can be used as a system-controlling parameter to tune the COP_c and the specific cooling power (SCP). The adsorber performs better when the regeneration time is 35% shorter than the adsorption time. The maximum COP_c occurs when the metal-adsorbent heat transfer coefficient reaches values of 100 $W.m^{-2}.K^{-1}$. The SCP greatly increases until this coefficient reaches 350 $W.m^{-2}.K^{-1}$. The adsorbent coating thickness severely influences the performance of an AC system. It was found that the maximum COP_c corresponds to a coating thickness of 1.75 mm and, the smaller the coating thickness the smaller the SCP. The metal tube's diameter and the HTF's velocity mainly influence the SCP since they have direct impact on the heat transfer rate exchanged between the HTF and the adsorbent material.

Keywords: Adsorption cooling; coated tube adsorber; adsorbent material; adsorbate vapor; cooling coefficient of performance (COP_c); specific cooling power (SCP).

Nomenclature

AC	Adsorption cooling
C	Specific heat ($J.kg^{-1}.K^{-1}$)
C_p	Constant pressure specific heat ($J.kg^{-1}.K^{-1}$)
COP_c	Cooling coefficient of performance
d	Diameter (m)
D_{ef0}	Effective diffusion coefficient ($m^2.s^{-1}$)
E_a	Activation energy ($J.kg^{-1}$)
HTF	Heat transfer fluid
$h_{f\rightarrow m}$	Fluid-metal convective heat transfer coefficient ($W.m^{-2}.K^{-1}$)
$h_{m\rightarrow s}$	Adsorbent-metal heat transfer coefficient ($W.m^{-2}.K^{-1}$)
k	Thermal conductivity ($W.m^{-1}.K^{-1}$)
k_0	Pre-exponential coefficient ($kg.kg^{-1}.Pa^{-1}$)
k_D	Blake-Kozeny permeability (m^2)
K_{LDF}	LDF constant (s^{-1})
L	Tube length (m)
m	Mass (kg)
P	Pressure (Pa)
Q	Heat (J)
q_m	Monolayer specific capacity ($kg.kg^{-1}$)
r	Radial coordinate (m)
R_p	Particle radius (m)
R'	Adsorbate specific gas constant ($J.kg^{-1}K^{-1}$)
SCP	Specific cooling power ($W.kg^{-1}$)
t	Time (s)
t_{SG}	Non-dimensional Toth constant
T	Temperature (K)
u	Adsorbate velocity ($m.s^{-1}$)
v	Velocity ($m.s^{-1}$)
X	Adsorbate concentration in the adsorbent ($kg_a.kg_s^{-1}$)
z	Axial longitudinal coordinate (m)

Subscripts

a	adsorbate
ads	adsorption
bed	adsorbent bed
c	condenser/cooling
cyc	cycle
e	evaporator
eq	equilibrium

f	fluid
h	heating
ic	isosteric cooling
ih	isosteric heating
in	inner
ini	initial
m	metal
max	maximum
min	minimum
out	outer
p	particle
reg	regeneration
s	adsorbent
v	vapor/vaporization

Greek letters

ΔH_{ads}	Adsorption heat ($J.kg^{-1}$)
ΔH_v	Heat of vaporization ($J.kg^{-1}$)
ε	Adsorbent bed porosity
μ	Dynamic viscosity (Pa.s)
ρ	Adsorbate density ($kg.m^{-3}$)
σ	Thickness (m)
τ	Cycle time (s)

1 Introduction

The global energy demand for space cooling has been increasing yearly by 6% for the residential sector (Palomba et al., 2017). Most of the cooling demands are fulfilled by conventional vapor compression cooling systems that rely on high global warming potential (GWP) refrigerants (HFCs and HCFCs). In addition, electrical energy is required to drive these systems, which contributes to the increase of greenhouse gases (GHG) emissions, since 43% of the gross electricity production is still obtained from fossil fuels combustion (European Environment Agency, 2018). In order to avoid catastrophic consequences of anthropogenic climate change 197 Parties signed the Paris Agreement, in which each party pledged to severely reduce greenhouse gases emissions (European-Commission, 2015). Therefore, the European Union aims to cut GHG emissions by 40% by 2030 relatively to the 1990 levels. Adsorption cooling (AC) technology is an environmentally friendly alternative to vapor compression systems. It works based on natural refrigerants with zero or nearly zero GWP such as water, ammonia, ethanol and methanol. Furthermore, AC systems are driven by thermal energy (solar, waste heat, biomass heat, natural gas, etc.), only requiring electricity to power small pumps and electronic control valves. As no moving parts are required for the refrigerant circulation, AC systems generate very low noise and no vibrations, making them appealing for quiet and household applications.

Combustible fuels (coal, oil, natural gas, biofuels, industrial and municipal waste, etc.) accounted for 66.8% of the total World gross electricity production in 2017 (International Energy Agency (IEA), 2019). Combustion's heat is used to produce steam driving electric generators through the spinning of steam turbines. This process is used in the majority of worldwide thermal power plants. Only

approximately 30% heat generated from the fuels' combustion is converted into electricity, being the remaining wasted heat (Kaushik et al., 2011). One of AC major limits is the low coefficient of performance (COP) when compared to the conventional vapor compression systems. Nonetheless, this should be carefully considered since it is commonly overrated. The COP for vapor compression systems is defined as the ratio between the thermal energy withdrawn (cooling production) and the electrical energy needed to drive the cooling system. However, when comparing an electrically driven system with a thermally driven one, it has to be noticed that 70% of the total heat is lost in its conversion to electricity, which also must be accounted for in electrically driven systems. Therefore, if the efficiency of electricity generation from heat is considered, the COP of compression refrigeration systems is much lower than the commonly reported one. In fact, from this perspective care is needed when comparing the COP of adsorption and vapor compression refrigeration systems, and the low COP of AC systems should not be considered such a huge disadvantage.

One of the most interesting features of AC systems is that they require heat to produce the cooling effect. In several cases, the need for cooling occurs when and where some excess heat exists, as waste heat from industrial processes and machine working, ambient heat, or solar heat. The thermal energy available can be used to drive AC systems by itself or to reduce the costs of the energy required to drive these systems. Advanced systems' configurations can be implemented in order to exploit the usage of available heat. Moreover, compressor dependent systems cannot provide cooling without electricity whereas AC systems can function resorting to very small batteries only to power their small pumps and electronic valves. Since most households do not have a backup electricity generator, an energy failure during an extreme hot period (like heat waves, which are becoming more intense and frequent) can bring disastrous consequences to human health and wellbeing. AC can help to overcome these situations, if driven by solar energy and resorting to very small batteries only.

A lot of research has been carried out over the last decade on AC technologies (Abd-Elhady and Hamed, 2020; Aristov, 2017; Mohammed et al., 2019; Vasta et al., 2018; Wang et al., 2010). Mohamed *et al.* carried out a scaling study of heat diffusion and vapor adsorption in an adsorbent silica gel packed bed (Mohammed et al., 2018). Valuable information on the influence of heat transfer resistances, intra and interparticle mass resistances, particle diameter and adsorbent thickness on the adsorbent bed performance was presented. Several studies are focused on the adsorbent-adsorbate working-pairs and their state equations, that can be used as database for future works (Elsayed et al., 2019; Hassan et al., 2015; Shmroukh et al., 2015; Younes et al., 2019, 2017). Mohamed and Askalany developed an advanced system that integrates adsorption cooling and desalination (Mohammed and Askalany, 2019). The studied cycle achieved a specific daily water production of 25 $kg_{water}/kg_{adsorbent}$. Frazzica *et al.* (Frazzica et al., 2016) built an adsorption refrigerator for air conditioning and refrigeration purposes, activated carbon and methanol being used as the working pair. The specific cooling power (SCP) achieved was 95 W/kg and 50 W/kg for air conditioning and refrigeration operating conditions, respectively. However, the achieved COP was in the range of 0.09-0.11, which is considerably low. In addition, the authors used a thermodynamic model to predict the COP and select the best adsorbent material. The COP predicted by the model, for the working pair used to build the prototype, was 0.63 and 0.55 respectively for air conditioning and refrigeration conditions, which are far from the considerably lower experimental results. From these results, it can be concluded that thermodynamic (equilibrium) models are not suitable to predict the performance of AC systems. In Ref. (Vodianitskaia et al., 2017) is presented an experimental adsorption chiller using the silica gel-water working pair. Grains of silica gel were packed in a finned tube heat exchanger. Different grain sizes were tested, and results showed that smaller grain sizes perform better considering the COP and SCP. The performance improvements obtained with smaller particle diameters have paved the way to the implementation of adsorbent coatings, which is

nowadays acknowledged as the most promising technique to achieve more performant adsorption systems (Dias and Costa, 2018). The enhancement of the SCP as a result of reducing particle diameter and bed thickness has also been reported in (Mohammed et al., 2017). Building AC systems with multiple adsorbent beds is also leading to improvements in the SCP (Rouf et al., 2020). An up-to-date review on performance enhancing techniques for adsorption air conditioning systems can be found in Ref. (Alahmer et al., 2019).

An interesting feature of the adsorption refrigeration is the capability of regenerating the adsorbent using solar thermal energy. Fernandes *et al.* (Fernandes et al., 2014) elaborated a comprehensive review on solar adsorption refrigeration systems. Given the low regeneration temperatures associated with silica gel, it has been a widely used adsorbent for solar adsorption refrigeration applications. A parametric analysis of a solar adsorption refrigerator was carried out by Brites *et al.* (Brites et al., 2016). The influence of several parameters on the overall system's performance was investigated. A prototype was developed and tested, and experimental results used to validate the numerical model. Among the many governing parameters, whose best numerical values need to be evaluated, are the adsorbent mass, the number of metallic fins in the adsorbent bed and the thermal contact resistance between the solar collector plate and the adsorbent. Recently, a silica gel-water adsorption air conditioning system has been developed and tested by Pan *et al.* (Pan et al., 2019). Experimental tests were carried out under different operating conditions. The study reported a cooling power of 3.98 kW and a COP_c of 0.63 operating with a regeneration temperature of 85.1 ^{o}C, a condenser temperature of 30.3 ^{o}C and an evaporator temperature of 22.8 ^{o}C. In addition, the authors reported that the water used to cool the adsorber can reach a temperature of 39.9 ^{o}C, making it suitable for domestic water pre-heating or heating purposes.

In order to improve the overall performance of AC systems, detailed numerical models enabling the identification of optimal values for the several governing parameters, configurations and designs are required. The increase of the computational capacities allows implementation of a higher level of detail in the numerical models, and detailed analyses of adsorption cooling systems.

This work considers a coated tube adsorber module, which was used for heating applications in previous works, and evaluates its performance when used for cooling purposes. The coated tube adsorber is presented as well as a physical model that has already been validated for heating purposes in previous studies (Dias and Costa, 2019; Zhang and Wang, 1999). Analysis of the impact of several governing parameters such as the evaporator, condenser and regeneration temperatures, cycle time, metal-adsorbent heat transfer coefficient (heat transfer coefficient between the outer tube wall and the adsorbent material), metal tube diameter, coating thickness and HTF's velocity on the adsorber's performance is performed. The reported results enable the identification of the key parameters and their best values for the use of the coated tube adsorber module in AC applications.

2 Coated tube adsorber

Coated tube adsorbers are nowadays considered the most promising configuration for adsorption applications (Dias and Costa, 2018), with the main advantages of high adsorbent-metal heat transfer coefficients and compact sizes. These improved characteristics have a significant impact on the cooling power of the AC systems due to more effective heat exchanges between the HTF and the adsorbent material. In addition, the compactness of the coated tube adsorbers allows the incorporation of higher adsorbent mass in smaller volumes.

Given the advantages of the coated tube design, a coated tube adsorber was selected for analysis in this paper. The adsorber consists on several cylindrical metal tubes, which outer surface is coated with the adsorbent material. These tubes are enclosed inside a sealed chamber, which is connected to the evaporator or condenser through several holes during adsorption and regeneration phases, respectively. Thus, adsorbate vapor flows from the evaporator to the chamber during the adsorption phase (heat release) and from the chamber to the condenser during the regeneration phase (heat reception). The HTF circulates inside the metal tubes in order to retrieve the heat released during the adsorption phase and provide heat to the adsorbent during the regeneration phase. The metal tubes are linked to two joints, which separate the adsorbate chamber from the HTF's inlet and outlet ports. The coated tube adsorber is depicted in Figure 1, which does not include all the tubes in order to keep the picture clear and perceptible.

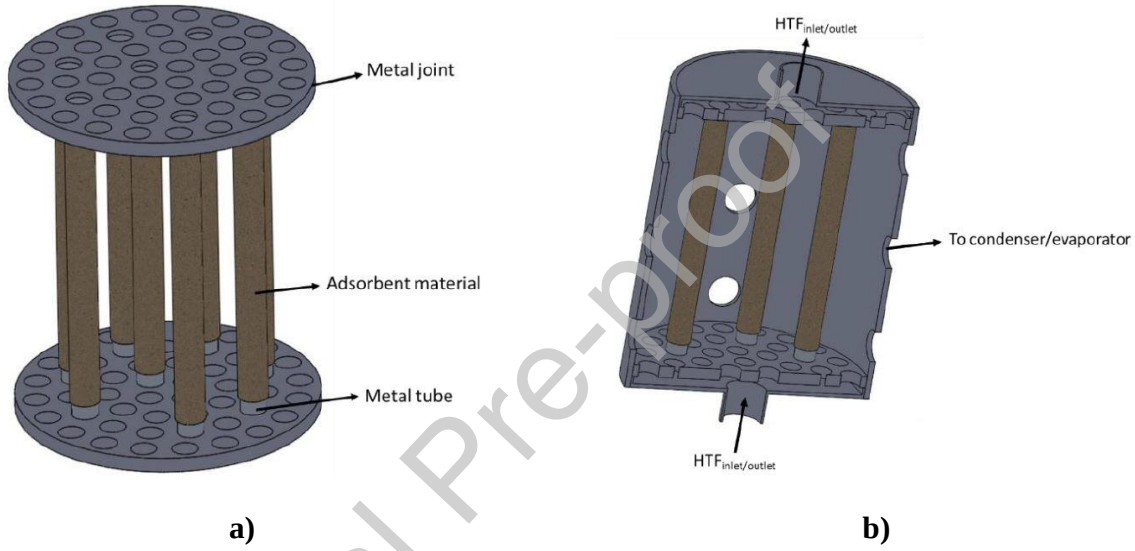

Figure 1 – **a)** Schematics of the adsorber module containing several metal tubes with an external adsorbent coating; **b)** Adsorber module cross section view. (Reproduced from (Dias and Costa, 2019) with permission from Elsevier).

Silica gel was used as adsorbent material due to its low regeneration temperature (<100 ºC), readiness to market, low cost, and good capacity of water adsorption, which was selected as adsorbate. The selected silica gel is of the RD2060 type from Fuji Silysia Chemical LTD. The silica gel is mixed with a binder to form an external coating on the metal tubes, improving the metal-adsorbent heat transfer coefficient and the coating thermal conductivity. The mass transfer resistance is increased by mixing the silica gel with the binder. However, since the coating thickness is small, mixing the adsorbent with the binder will have more benefits than hindrances on the system's performance (Frazzica et al., 2014).

3 Adsorber model

This work implemented a two-dimensional distributed parameter model. The implemented model resorts on general mass and energy conservation laws, and on particular constitutive laws and thermophysical properties that are well documented and that were previously validated. Although the situation/system presented in this work is different, the constitutive laws and thermophysical properties, as well as the adsorption data, remain the same for each particular adsorbent-adsorbate working pair, which makes the model a validated tool that can be applied for adsorption systems in

general. Since the geometry is symmetric over the angular direction, only the radial and axial coordinate directions are considered. This model was studied in a previous work, where it was found which dimensional model must be used for the analysis of the coated tube adsorber for adsorption heat pumps (Dias and Costa, 2019). Although lumped parameter models can accurately predict the COP of a coated tube adsorber under particular scenarios, that study concluded that the implementation of a two-dimensional distributed parameter model is necessary to achieve accurate predictions for the specific heating power. As all adsorber tubes are equal, the physical model describes the dynamics of a single representative tube only, and the overall results depend on the adsorber's number of tubes. The representative metal tube with the external adsorbent coating and its schematics are presented in Figure 2.

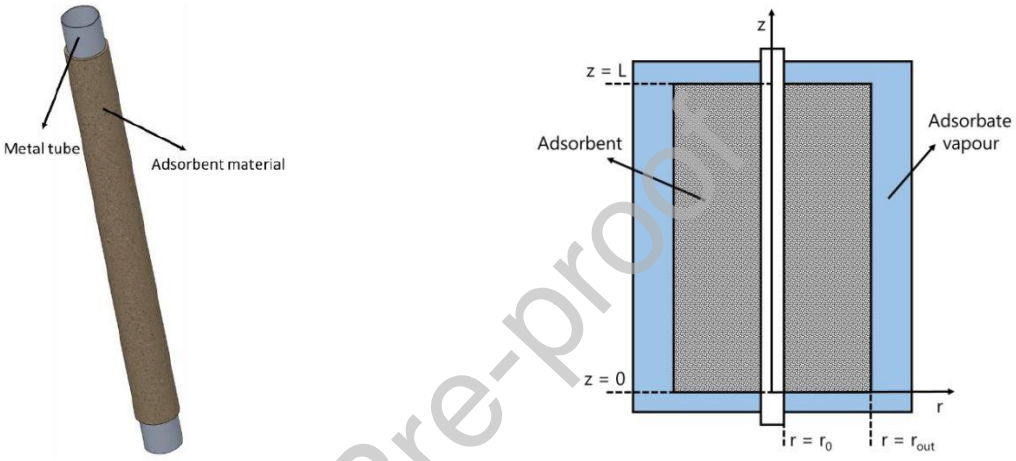

a) **b)**

Figure 2 – a) Representative metal tube externally coated with the adsorbent material; **b)** Coated tube schematics. (Reproduced from (Dias and Costa, 2018) with permission from Elsevier).

The implemented model results from the application of the energy and mass balance equations to the coated tube geometry, respectively Equations (1) and (2):

$$\frac{\partial(\rho C_p T_s)}{\partial t} + \nabla(\rho_v C_{p,v} T_s u) - \nabla(k_s \nabla T_s) - \rho_s(1-\varepsilon)\Delta H_{ads}\frac{\partial X}{\partial t} = 0 \quad (1)$$

$$\varepsilon\frac{\partial \rho_v}{\partial t} + \nabla(\rho_v u) + \rho_s(1-\varepsilon)\frac{\partial X}{\partial t} = 0 \quad (2)$$

where

$$\rho C_p = \varepsilon\rho_v C_{p,v} + \rho_s(1-\varepsilon)(C_s + X C_{p,a}) \quad (3)$$

and

$$\boldsymbol{\varepsilon = \varepsilon_{bed} + (1 - \varepsilon_{bed})\varepsilon_p} \tag{4}$$

Darcy's Law is used to express the momentum balance

$$\boldsymbol{u = -\frac{k_D}{\mu}\nabla P} \tag{5}$$

and the Blake-Kozeny model is used to obtain the adsorbent bed permeability (Wilkes and Birmingham, 2006)

$$\boldsymbol{k_D = \frac{d_p^2 \varepsilon_{bed}^3}{150(1 - \varepsilon_{bed})^2}} \tag{6}$$

The linear driving force (LDF) model is adopted to describe the adsorbate uptake (Sircar, 1983):

$$\boldsymbol{\frac{dX}{dt} = K_{LDF}(X_{eq} - X)} \tag{7}$$

where K_{LDF} coefficient can be obtained as:

$$\boldsymbol{K_{LDF} = \frac{15 D_{ef0} e^{-\frac{E_a}{R' T_s}}}{R_p^2}} \tag{8}$$

For the silica gel-water working pair, the adsorbate concentration in the adsorbent at equilibrium, X_{eq}, can be obtained as:

$$\boldsymbol{X_{eq} = \frac{P k_0 e^{\frac{\Delta H_{ads}}{R' T_s}}}{\left[1 + \left(\frac{P k_0}{q_m} e^{\frac{\Delta H_{ads}}{R' T_s}}\right)^{t_{SG}}\right]^{\frac{1}{t_{SG}}}}} \tag{9}$$

The physical model is implemented considering the following main assumptions:

- Adsorbent bed is homogenous;
- The evaporator and the condenser are ideal heat exchangers with uniform internal pressures;
- Adsorbate vapor phase behaves as an ideal gas and the adsorbed phase is considered to be liquid;
- Specific heats of the adsorbate vapor and liquid phases are constants;
- Adsorbate vapor around the adsorbent is always in the saturation conditions;
- Thermophysical properties of solid materials do not change with temperature;

- Temperature and pressure in the adsorbent bed are uniform along the angular direction;

The adsorbate uptake is obtained through the LDF model, Equation (7), and it depends on the pressure and temperature along the adsorbent bed, $P(r,z)$ and $T(r,z)$. The energy conservation equation for the adsorbent bed can be written as:

$$\begin{aligned}\left[\boldsymbol{\rho_s(1-\varepsilon)(C_s+XC_l)+\varepsilon\rho_v C_{p_v}}\right]\frac{\boldsymbol{dT_s}}{\boldsymbol{dt}} = \\ = (\mathbf{1}-\boldsymbol{\varepsilon})\boldsymbol{\rho_s}\Delta\boldsymbol{H_{ads}}\frac{\boldsymbol{dX}}{\boldsymbol{dt}}+\frac{\boldsymbol{k_s}}{\boldsymbol{r}}\left(\frac{\boldsymbol{\partial T_s}}{\boldsymbol{\partial r}}+\boldsymbol{r}\frac{\boldsymbol{\partial^2 T_s}}{\boldsymbol{\partial r^2}}\right) \\ -\frac{\boldsymbol{C_{p_v}}}{\boldsymbol{r}}\left(\boldsymbol{\rho_v T_s u_r}+\boldsymbol{r T_s u_r}\frac{\boldsymbol{\partial\rho_v}}{\boldsymbol{\partial r}}+\boldsymbol{r\rho_v u_r}\frac{\boldsymbol{\partial T_s}}{\boldsymbol{\partial r}}+\boldsymbol{r\rho_v T_s}\frac{\boldsymbol{\partial u_r}}{\boldsymbol{\partial r}}\right) \\ -\boldsymbol{C_{p_v}}\left(\boldsymbol{T_s u_z}\frac{\boldsymbol{\partial\rho_v}}{\boldsymbol{\partial z}}+\boldsymbol{\rho_v T_s}\frac{\boldsymbol{\partial u_z}}{\boldsymbol{\partial z}}+\boldsymbol{\rho_v u_z}\frac{\boldsymbol{\partial T_s}}{\boldsymbol{\partial z}}\right)+\boldsymbol{k_s}\left(\frac{\boldsymbol{\partial^2 T_s}}{\boldsymbol{\partial z^2}}\right)\end{aligned} \tag{10}$$

For the mass conservation, Equation (2) can be rearranged as:

$$\begin{aligned}\frac{\boldsymbol{\partial\rho_v}}{\boldsymbol{\partial t}} = -\frac{\mathbf{1}}{\boldsymbol{\varepsilon}}\Big[\boldsymbol{\rho_s}(\mathbf{1}-\boldsymbol{\varepsilon})\Delta\boldsymbol{H_{ads}}\frac{\boldsymbol{\partial X}}{\boldsymbol{\partial t}}+\frac{\mathbf{1}}{\boldsymbol{r}}\Big(\boldsymbol{r u_r}\frac{\boldsymbol{\partial\rho_v}}{\boldsymbol{\partial r}}+\boldsymbol{\rho_v r}\frac{\boldsymbol{\partial u_r}}{\boldsymbol{\partial r}}+\boldsymbol{\rho_v u_r}\Big) \\ +\boldsymbol{\rho_v}\frac{\boldsymbol{\partial u_z}}{\boldsymbol{\partial z}}+\boldsymbol{u_z}\frac{\boldsymbol{\partial\rho_v}}{\boldsymbol{\partial z}}\Big]\end{aligned} \tag{11}$$

Since $r_{tube} \ll L_{tube}$, the HTF temperature variation along the radial coordinate can be neglected, $\frac{\partial T_f}{\partial r} \approx 0$. As the HTF velocity is constant, the energy balance equation for the HTF is:

$$\boldsymbol{\rho_f C_{p,f}}\frac{\boldsymbol{\partial T_f}}{\boldsymbol{\partial t}} = \boldsymbol{k_f}\left(\frac{\boldsymbol{\partial^2 T_f}}{\boldsymbol{\partial z^2}}\right)-\boldsymbol{u_f\rho_f C_{p,f}}\frac{\boldsymbol{\partial T_f}}{\boldsymbol{\partial z}}+\frac{\boldsymbol{4h_{f\to m}}}{\boldsymbol{d_{in}}}\left(\boldsymbol{T_m}-\boldsymbol{T_f}\right) \tag{12}$$

The temperature of the metal tube is considered constant along the radial direction due to the small thickness and metal's high thermal conductivity, $\frac{\partial T_m}{\partial r} \approx 0$. The energy balance equation for the metal tube is given by:

$$\boldsymbol{\rho_m C_m}\frac{\boldsymbol{dT_m}}{\boldsymbol{dt}} = \boldsymbol{k_m}\left(\frac{\boldsymbol{\partial^2 T_m}}{\boldsymbol{\partial z^2}}\right)+\frac{\boldsymbol{4d_{in}h_{f\to m}(T_f-T_m)}}{\boldsymbol{d_{out}^2-d_{in}^2}}+\frac{\boldsymbol{4d_{out}h_{m\to s}(T_s-T_m)}}{\boldsymbol{d_{out}^2-d_{in}^2}} \tag{13}$$

The partial differential equation's system is solved using the method of lines by discretizing the derivatives in the radial and axial coordinates using the finite difference method. The resultant system of ordinary differential equations is solved resorting to the Matlab R2018b ode15s solver. The initial conditions used to obtain the presented results are:

$$t_{ini} = 0 \qquad P(t_{ini}) = P_{ini}$$

$$T_m(t_{ini}) = T_f(t_{ini}) = T_s(t_{ini}) = T_{ini} \qquad X(t_{ini}) = X_{eq}(P_{ini}, T_{s_{ini}})$$

The temperature and pressure boundary conditions used to solve the model's equations are as follows:

$$\left.\frac{\partial P}{\partial r}\right|_{r=r_0} = 0$$

$$P|_{r=r_{out}} = P|_{z=0} = P|_{z=L} = P_e, \qquad Adsorption$$

$$P|_{r=r_{out}} = P|_{z=0} = P|_{z=L} = P_c, \qquad Regeneration$$

$$\left.\frac{\partial P}{\partial r}\right|_{r=r_{out}} = \left.\frac{\partial P}{\partial r}\right|_{z=0} = \left.\frac{\partial P}{\partial r}\right|_{z=L} = 0, \qquad Cooling/Heating$$

$$-k_s \left.\frac{\partial T_s}{\partial r}\right|_{r=r_0} = h_{m\to s}(T_m - T_s)$$

$$\left.\frac{\partial T_s}{\partial r}\right|_{r=r_{out}} = \left.\frac{\partial T_s}{\partial z}\right|_{z=0} = \left.\frac{\partial T_s}{\partial z}\right|_{z=L} = 0$$

$$T_f|_{z=0} = T_{ads}, \qquad Adsorption/Cooling$$

$$T_f|_{z=0} = T_{reg}, \qquad Regeneration/Heating$$

$$\left.\frac{\partial T_f}{\partial z}\right|_{z=L} = 0$$

$$\left.\frac{\partial T_m}{\partial z}\right|_{z=0} = \left.\frac{\partial T_m}{\partial z}\right|_{z=L} = 0$$

The physical model is described with extensive detail in reference (Dias and Costa, 2019).

4 Results and discussion

The coated tube adsorber's performance is investigated considering several parameters, which are suitable for cooling applications such as air conditioning and water chillers. The adsorber's performance is analyzed resorting on the cooling coefficient of performance (COP_c) and the specific cooling power (SCP), defined respectively as:

$$COP_c = \frac{Q_e}{Q_{ih} + Q_{reg}} \tag{14}$$

$$SCP = \frac{Q_e}{m_s \tau_{cyc}} \tag{15}$$

Heats provided during the isosteric heating (Q_{ih}) and regeneration (Q_{reg}) are calculated through Equations (16) and (17), respectively:

$$Q_{ih} \approx \int_{T_{initial}}^{T_{final}} \left[m_s\left(C_s + X_{max}C_{p,a}\right) + m_m C_m\right] dT \tag{16}$$

$$Q_{reg} \approx \int_{T_{initial}}^{T_{final}} \left[m_s\left(C_s + XC_{p,a}\right) + m_m C_m\right] dT - \int_{X_{max}}^{X_{min}} m_s \Delta H_{ads} dX \tag{17}$$

where the $T_{initial}$ and T_{final} refer the initial and final temperatures of the isosteric heating and regeneration phases, respectively. Finally, the heat drawn by the evaporator (Q_e), which is the useful cooling effect, is obtained as:

$$Q_e = m_s \Delta X \Delta H_v + \int_{T_c}^{T_e} m_s \Delta X C_{p,a} dT \tag{18}$$

where T_c and T_e are the condenser and evaporator temperatures, respectively. The influence of the evaporator, condenser and regeneration temperatures, cycle times, metal-adsorbent heat transfer coefficient, metal tube diameter, coating thickness and HTF's velocity on the COP_c and SCP of the coated tube adsorber are analyzed. A set of reference parameters suitable for cooling applications was selected, which is summarized in Table 1. Throughout the analyses, one parameter is varied at a time whilst the others assume their reference values (segregated approach).

Table 1 – *Parameters used as references.*

Parameter	Value	Unit
C_m	910	J.kg^{-1}.K^{-1}
C_s	921	J.kg^{-1}.K^{-1}
d_p	3.5×10^{-4}	m
$d_{in,tube}$	0.01	m
E_a	2.3314×10^{6}	J.kg^{-1}
$h_{m \to s}$	200	W.m^{-2}.K^{-1}
k_0	7.3×10^{-13}	kg.kg^{-1}.Pa^{-1}
k_f	0.6	W.m^{-1}.K^{-1}
k_m	205	W.m^{-1}.K^{-1}
k_s	0.198	W.m^{-1}.K^{-1}
L_{tube}	1	m
ΔH_v	2.3×10^{6}	J.kg^{-1}
q_m	0.45	kg.kg^{-1}
R_p	1.75×10^{-4}	m
t_{ads}	600	s
T_c	$273.15 + 22$	K
T_e	$273.15 + 10$	K
$T_{f,ads}$	$273.15 + 20$	K
$T_{f,reg}$	$273.15 + 90$	K
t_{reg}	$0.91 \times t_{ads}$	s
t_{SG}	12	-
v_{HTF}	0.05	m.s^{-1}
ΔH_{ads}	2.693×10^{6}	J.kg^{-1}
ε_{bed}	0.4	-
ρ_m	2700	Kg.m^{-3}
ρ_s	2027	Kg.m^{-3}
σ_s	0.002	m
σ_{tube}	0.001	m

4.1 Evaporator temperature

The evaporator temperature directly determines the adsorber's pressure during the adsorption phase. The adsorber's performance was evaluated for evaporator temperatures in the 0-20 ºC range, suitable for several cooling applications. The influence of the evaporator temperature on the COP_c and SCP is represented in Figure 3. As expected, for higher evaporator temperatures the COP_c and the SCP increase. The performance decreases for low evaporator temperatures due to the lower pressure during adsorption, which results in lower adsorption capacity. Thus, low evaporator temperatures cause reduced refrigerant flowing in each cycle. In order to reduce the pressure inside the adsorber, the adsorber must be cooled down. The temperature of the cooling HTF dictates the lowest pressure that can be reached in the adsorbent bed. Therefore, if the temperature of the cooling HTF is not low enough, the adsorber cannot be sufficiently cooled down to reach the reduced evaporator pressure, precluding the adsorbate adsorption. Therefore, the temperature of the HTF cooling fluid will limit

the lowest pressure that can be reached in the adsorber and, consequently, the lowest evaporator temperature (relevant for producing the useful cooling effect) for the system's proper operation.

It might seem that setting $T_e = T_c$ would not make sense as no heat transfer occurs for equal temperatures. However, the system's evolution is unsteady, the implemented model is dynamic, and the evaporator and condenser pressures are equal just at the beginning of each cycle. Although the adsorption and regeneration phases are theoretically isobaric, in practice the pressure during adsorption phase is lower that the initial P_e and the pressure during regeneration phase is higher than P_c. Consequently, the evaporator and condenser temperatures over each cycle are respectively lower and higher than the operating conditions set at the beginning of each cycle. Although not represented in Figure 3, it is possible to evaluate non-zero adsorber's performance for $T_e = T_c$, which are only equal at the initial instant of each cycle.

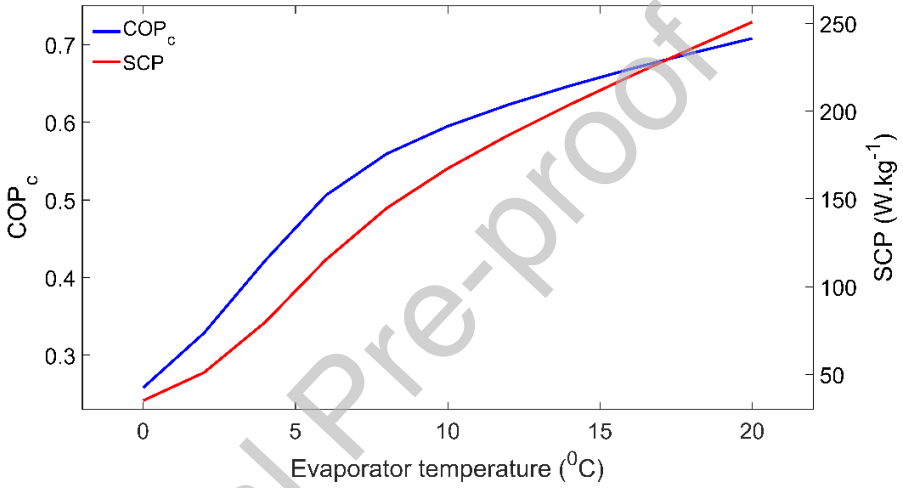

Figure 3 – Influence of the evaporator temperature on the adsorber's performance.

4.2 Condenser temperature

The adsorber's pressure during the regeneration phase is set by the condenser temperature. Simulations were carried out considering that the condenser would reject heat in a temperature range of 15-41 ºC. The effect of the condenser temperature on the adsorber's performance is presented in Figure 4. Both COP_c and SCP are reduced when the condenser temperature increases, which is inherent to both adsorption and conventional cooling systems. The decrease of the SCP is almost linear; however, with the increase of the condenser temperature the decrease of COP_c becomes more abrupt. This is due to the pressure increase during the regeneration phase for higher condenser temperatures, which increases the amount of adsorbate in the adsorbent for the same regeneration temperature. In a limit scenario, if the regeneration temperature is not high enough to increase the adsorber's pressure to the level of the condenser pressure, the adsorbent material is not regenerated.

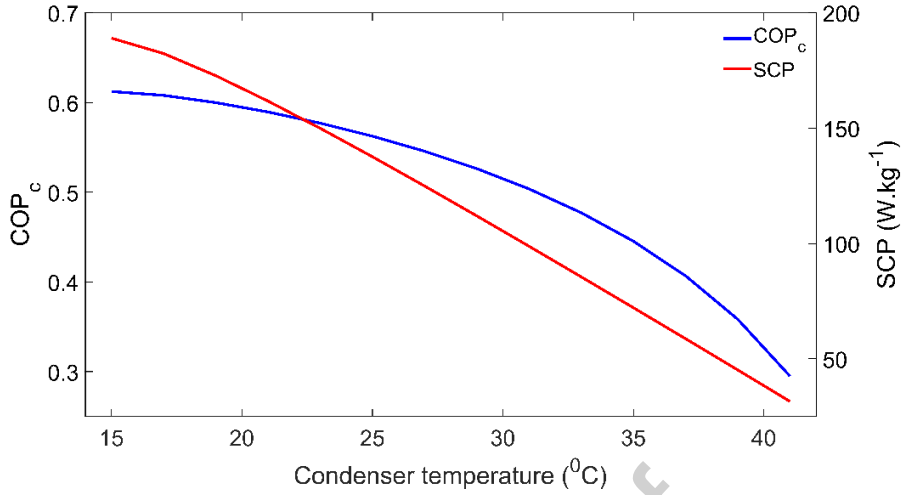

Figure 4 – Effect of the condenser temperature on the adsorber's performance.

4.3 Regeneration temperature

The required regeneration temperature highly depends on the adsorbent-adsorbate working pair. For the investigated working pair, silica gel-water, regeneration temperatures between 60 ºC and 90 ºC are commonly used. In this work, the adsorber's performance was evaluated for regeneration temperatures in the 50-90 ºC range. The COP_c and SCP as a function of the regeneration temperature are represented in Figure 5. The COP_c reaches its maximum for a regeneration temperature of approximately 70 ºC. According to these results, from the energy output/input ratio, it is not worth to regenerate the adsorbent with temperatures higher than 75 ºC, since the adsorbate flow increase does not compensate the additional energy input required to heat the HTF up to 90 ^{o}C. Concerning the SCP, its value increases with the regeneration temperature since higher regeneration temperatures result on faster heat transfer (higher heat transfer rate) between the HTF and the adsorbent material. Since water is used as HTF, regeneration temperatures higher than 90 ºC were not considered, preventing boiling and the use of a pressurized system, including safety devices like a pressure relief valve.

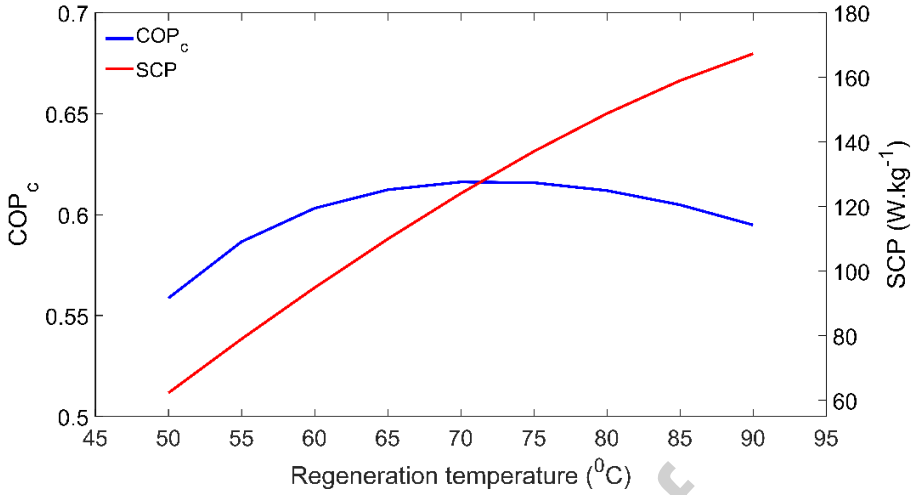

Figure 5 – COP_c and SCP as function of the regeneration temperature.

4.4 Cycle time

The cycle time is one of the most relevant parameters since it directly controls the system dynamics. The cycle time depends on the adsorption time set for each simulation. The adsorption time was varied from 50 s up to 3000 s, resulting on the cycle times that are the abscissas of Figure 6, demonstrating its relevance on the adsorber's performance. When the cycle time is too low, COP_c and SCP are minimal since there is not enough time for heat exchange between the adsorbent material and the HTF, resulting in an almost zero adsorbate flow. However, for longer cycle times COP_c and SCP present opposite behaviors. As the cycle time increases, the COP_c also increases reaching a maximum for the highest cycle times, as long cycle times allow the maximum adsorption capacity to be reached for a given combination of temperature and pressure. On the other hand, the SCP reaches its peak for a cycle time of approximately 17 min and significantly decreases for longer cycle times. Longer cycle times allow higher COP_c (more complete heat and mass transfers), but only few cycles by unit time, and thus lower powers. The right balance between the COP_c and the SCP must be selected, depending on the priority for the AC system to provide more power (higher SCP) or to have a higher energy performance (higher COP_c).

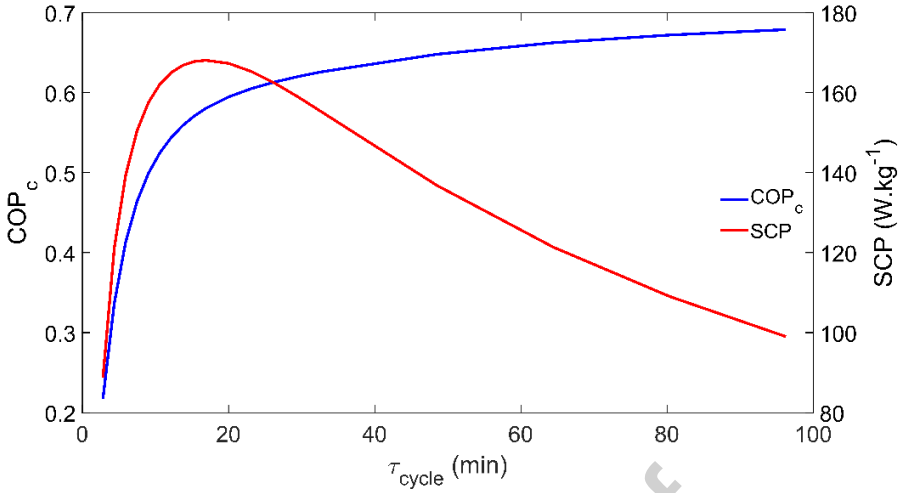

Figure 6 – Influence of the cycle time on the adsorber's performance.

4.5 Regeneration time

Regeneration phase is normally faster than the adsorption phase. In addition, the regeneration phase of an adsorption system occurs when the major (driving) energy is provided to the system. In Figure 7is presented the influence of the regeneration time on the adsorber's performance. The regeneration time is taken as a fraction of the adsorption time. By analyzing these results, it can be seen that the COP_c is not significantly affected by reducing the regeneration time. Although the SCP shows a peak when the regeneration phase lasts for 65% of the adsorption time, it does not reflect severe variations as occurring for other parameters. Nonetheless, if a large mass of adsorbent material is used, small changes on the SCP will result on significant changes on the system's (absolute) cooling power.

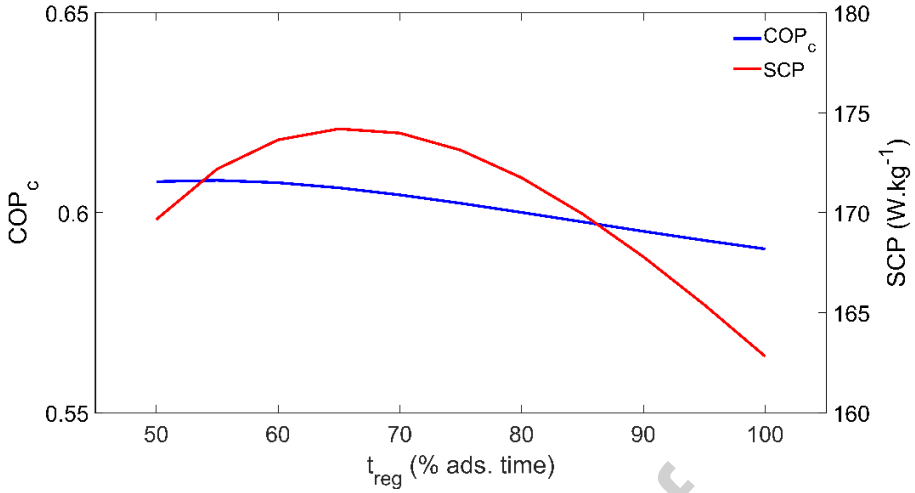

Figure 7 – Effect of the regeneration time on the adsorber's performance.

4.6 Tube-adsorbent heat transfer coefficient

The heat transfer between the external metal wall and the adsorbent coating has major influence on the adsorber's performance. This is the main reason for the use of coatings over granular beds. Value of this heat transfer coefficient is hard to measure and, and it is commonly estimated or used as a calibration parameter for the simulation models. Applying a thermal paste to the external metal tube's wall enables higher metal-adsorbent heat transfer coefficients. Values higher than 400 W.m-2.K-1 have been reported in the literature for adsorbent coatings (Frazzica et al., 2014; Restuccia et al., 2002). Simulations were carried out varying this parameter from 25 $W.m^{-2}.K^{-1}$ up to 600 $W.m^{-2}.K^{-1}$ and the results are presented in Figure 8. Both COP_c and SCP greatly increase with the metal-adsorbent heat transfer coefficient, for lower values of this coefficient. Increasing this coefficient beyond 100 $W.m^{-2}.K^{-1}$ will not have significant impact on the COP_c. However, in order to obtain the highest SCP this coefficient should be at least 350 $W.m^{-2}.K^{-1}$. Further increase of this heat transfer coefficient will have only an insignificant impact on the system's performance.

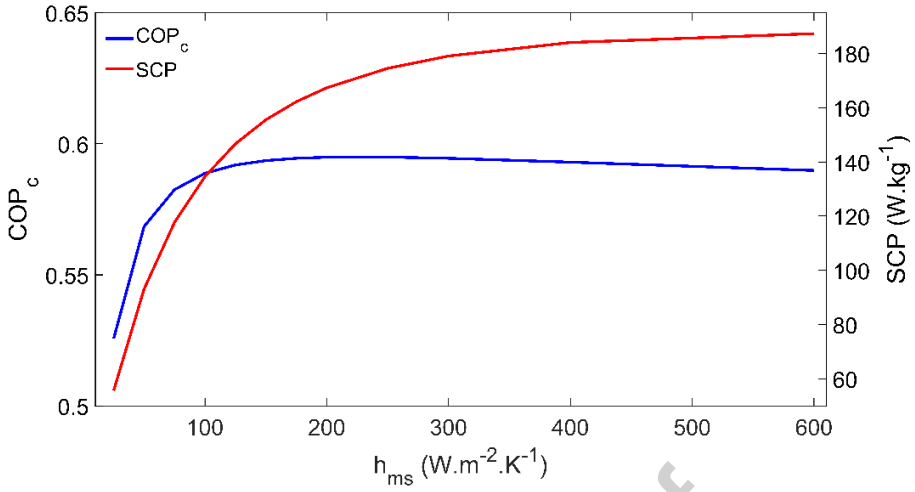

Figure 8 – Tube-adsorbent heat transfer coefficient's impact on the adsorber's performance.

4.7 Adsorbent coating thickness

Thickness of the adsorbent coating is very important for the adsorber's design since it will not only influence the COP_c and the SCP, but also the mass of adsorbent material coating each metal tube (and thus the total mass of adsorbent material in the adsorber). Figure 9 depicts the adsorber's performance as function of the adsorbent coating thickness. Results show that coating thicknesses higher than 3 mm lead to very low values of COP_c and SCP. The COP_c reaches its maximum for a thickness of approximately 1.75 mm, whereas the SCP is highest for the lowest coating thickness. Given the inverse behavior of these two performance coefficients, the thickness of the adsorbent coating must be selected accordingly to the AC system application. If the maximum COP_c is desired, the adsorbent coating thickness should be in the range of 1.5-2 mm; however, if high SCP is preferable, the coating thickness must be smaller. Nevertheless, caution must be taken when greatly reducing the adsorbent coating thickness since the mass of adsorbent coating each metal tube will be tiny, which may require an impracticable number of tubes to achieve the demanded total (absolute) cooling power.

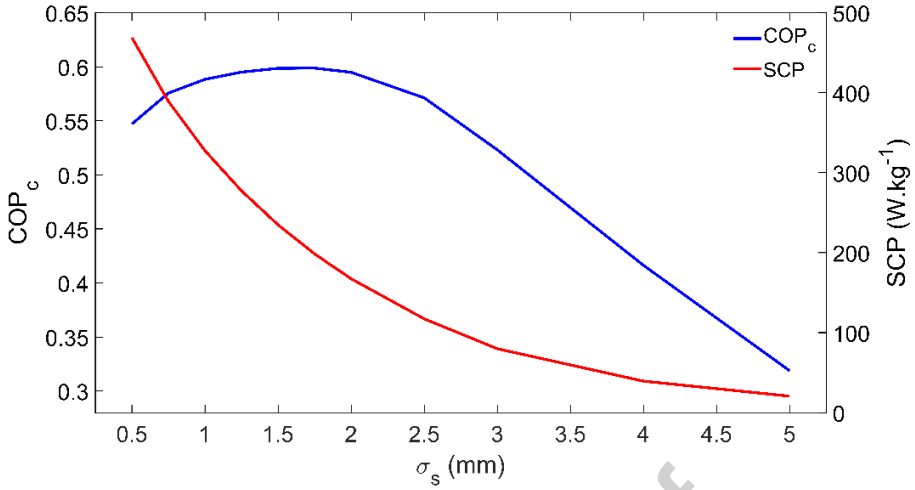

Figure 9 – Adsorber's performance as function of the adsorbent coating thickness.

4.8 Tube diameter

The tube's diameter, conjugated with the coating thickness, has a direct influence on the amount of adsorbent material coating each tube and on the contact area between the adsorbent coating and the tube wall. The tube's inner diameter was varied from 5 mm up to 70 mm. The velocity of the HTF was kept constant, resulting on different mass flow rates for the different tube diameters. The adsorber's performance for the different tube diameters tested is presented in Figure 10. First, a noticeable performance increase occurs for diameters over 35 mm due to the HTF flow regime transition from laminar to turbulent. The COP_c is not significantly affected by the changes on the tube's diameter. Under the HTF laminar flow conditions, the SCP is highest for a diameter of 10 mm, resulting from the best combination between the HTF mass flow rate and the adsorbent coating mass. Shifting to turbulent flow regime, the HTF mass flow rate is sufficient to provide/withdraw heat to/from the adsorber, and the influence of the tube's diameter on the adsorber's performance becomes insignificant. Meanwhile, it might be counterproductive to use large tube diameters since it will result in large adsorbers containing low adsorbent mass, which may become too large and impracticable if medium to high cooling powers are required.

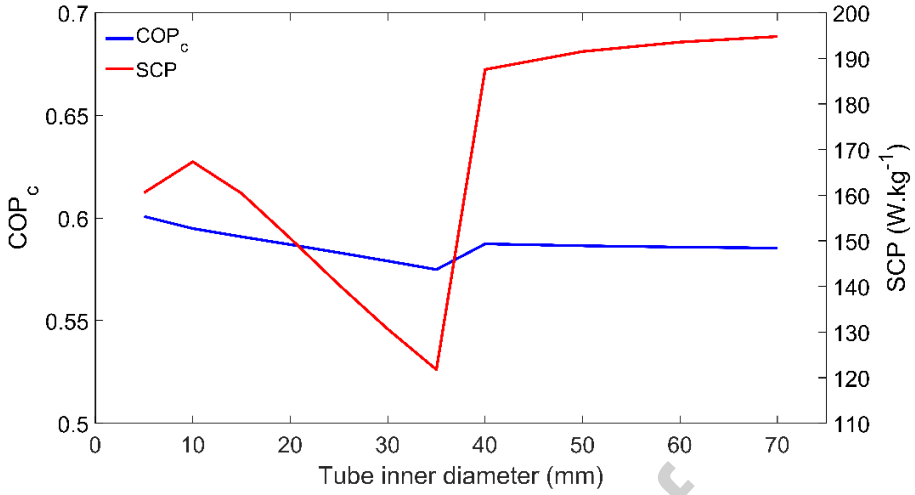

Figure 10 – Influence of the tube's diameter on the adsorber's performance.

4.9 Heat transfer fluid velocity

At last, the influence of the HTF's velocity on the adsorber's performance was investigated and the results presented in Figure 11. The COP_c does not present significant changes for the tested flow velocities since the adsorption and regeneration temperatures did not change. On the other hand, as the HTF's velocity directly influences the heat exchange inside the adsorber, it will affect the system's SCP. The SCP greatly increases with the flow velocity in the velocity range 0.005 $m.s^{-1}$ up to 0.02 $m.s^{-1}$, moderately increases in the velocity range 0.02 $m.s^{-1}$ up to 0.04 $m.s^{-1}$, and for HTF velocities beyond 0.04 $m.s^{-1}$ only residually changes, meaning that for these highest HTF velocities the adsorption kinetics becomes the limiting factor. For cooling applications, the HTF's velocity should be high enough so that the limits for the heat transfer in the adsorber are dictated by the adsorption kinetics of the selected working pair, guaranteeing it is not the HTF's velocity the performance limiting factor.

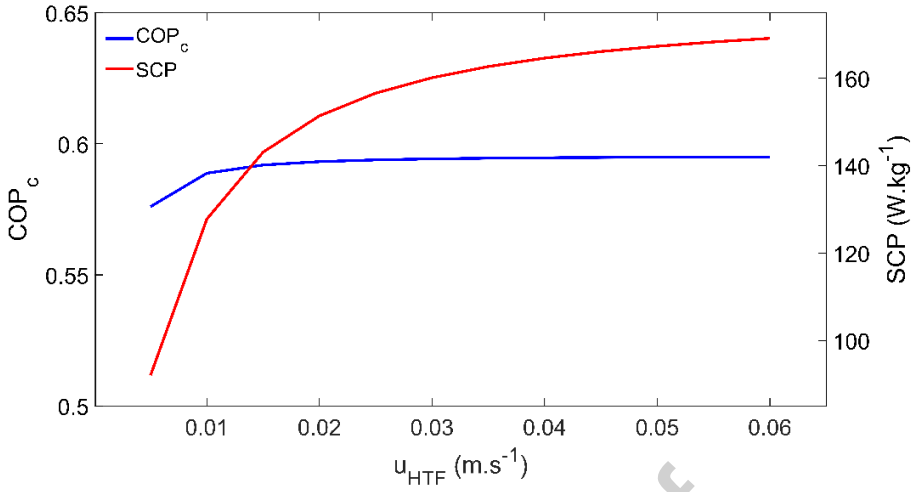

Figure 11 – HTF's velocity impact on the adsorber's performance.

5 Conclusions

The influence of several governing parameters on the performance of a coated tube adsorber for cooling applications was numerically analyzed. Some results were already anticipated, such as better adsorber's performance for higher evaporator temperatures and lower condenser temperatures. Nevertheless, a detailed characterization enables the better tuning of an AC system, whose behavior is inherently unsteady. Higher regeneration temperatures result in higher cooling powers, although the highest COP_c occurs when using a regeneration temperature of approximately 70 ºC. Despite the fact that long cycle times allow maximum COP_c, the SCP becomes low or even very low. The cycle time must be carefully selected in order to provide the best combination between the COP_c and the SCP for each specific application of the AC system. Use of a regeneration time close to 65% of the adsorption time allows the best performance for the tested coated tube adsorber.

The external tube wall-adsorbent coating heat transfer coefficient should be higher than 100 $W.m^{-2}.K^{-1}$ in order to provide satisfactory SCP. The highest COP_c and SCP occur when this heat transfer coefficient has values of 100 $W.m^{-2}.K^{-1}$ and 350 $W.m^{-2}.K^{-1}$, respectively. An adsorbent coating thickness of approximately 1.75 mm will allow the highest COP_c; however, the SCP is higher for the smaller coating thicknesses. Although these results might suggest the use of small coating thicknesses to obtain high SCP values, decreasing the coating thickness excessively means that only a small mass of adsorbent is coating each tube, which may require a large number of tubes to achieve the required (absolute) cooling power. The tube's inner diameter must be carefully selected as it influences the adsorbent mass per tube, the contact area between the external tube wall and the adsorbent coating, and the HTF mass flow rate. While under laminar flow regime, simulations suggest that an inner diameter of 10 mm is the best solution. When the inner tube diameter is high enough for HTF turbulent flow to develop, further increase on the tube diameter has an insignificant impact on the adsorber's performance. Increasing the HTF's velocity causes minimal improvements on the COP_c. Nonetheless, its increase until approximately 0.03 $m.s^{-1}$ leads to higher SCP, but no further significant changes on the system's performance are observed if the HTF velocity increases above 0.03 $m.s^{-1}$.

Generally, the working temperatures have major influence on the COP_c, a well-known main message from Thermodynamics. However, due to the unsteady nature of the involved processes, only dynamic studies of this type can provide detailed information on how they influence the AC systems' performance. On the other hand, parameters related to the cycle duration or to the heat transfer between the adsorbent material and the HTF have a major impact on the SCP. Longer cycle times allow more complete heat and mass transfers, and thus higher COP_c. However, longer cycle times allow only a lower number of cycles by unit time, and thus lower SCP. Thus, a balance of these two performance parameters is required for the best performance of a coated tube adsorber, depending on the specific AC application. The additional balance between the investment and working costs of each AC system can provide the additional information needed to set the better COP_c and SCP combination.

Acknowledgements

The authors acknowledge the Portuguese Foundation for Science and Technology (FCT) for the financial support provided through the grant SFRH/BD/145124/2019, the project UID/EMS/00481/2013-FCT and CENTRO-01-0145-FEDER-022083.

The present study was developed in the scope of the Smart Green Homes Project [POCI-01-0247-FEDER-007678], a co-promotion between Bosch Termotecnologia S.A. and the University of Aveiro. It is financed by Portugal 2020 under the Competitiveness and Internationalization Operational Program, and by the European Regional Development Fund.

References

Abd-Elhady, M.M., Hamed, A.M., 2020. Effect of fin design parameters on the performance of a two-bed adsorption chiller. Int. J. Refrig. https://doi.org/10.1016/j.ijrefrig.2020.01.006

Alahmer, A., Ajib, S., Wang, X., 2019. Comprehensive strategies for performance improvement of adsorption air conditioning systems : A review. Renew. Sustain. Energy Rev. 99, 138–158. https://doi.org/10.1016/j.rser.2018.10.004

Aristov, Y.I., 2017. Adsorptive transformation and storage of renewable heat: Review of current trends in adsorption dynamics. Renew. Energy 110, 105–114. https://doi.org/10.1016/j.renene.2016.06.055

Brites, G.J.V.N., Costa, J.J., Costa, V.A.F., 2016. Influence of the design parameters on the overall performance of a solar adsorption refrigerator. Renew. Energy. https://doi.org/10.1016/j.renene.2015.07.099

Dias, J.M.S., Costa, V.A.F., 2019. Which dimensional model for the analysis of a coated tube adsorber for adsorption heat pumps? Energy 174, 1110–1120. https://doi.org/10.1016/J.ENERGY.2019.03.028

Dias, J.M.S., Costa, V.A.F., 2018. Adsorption heat pumps for heating applications: A review of current state, literature gaps and development challenges. Renew. Sustain. Energy Rev. 98, 317–327. https://doi.org/10.1016/J.RSER.2018.09.026

Elsayed, E., AL-Dadah, R., Mahmoud, S., Anderson, P., Elsayed, A., 2019. Adsorption cooling system employing novel MIL-101(Cr)/CaCl2 composites: Numerical study. Int. J. Refrig. https://doi.org/10.1016/j.ijrefrig.2019.08.004

European-Commission, 2015. Paris Agreement | Climate Action. Eur. Comm. Clim. Action.

European Environment Agency, 2018. Overview of electricity production and use in Europe [WWW Document]. URL https://www.eea.europa.eu/data-and-maps/indicators/overview-of-the-electricity-production-2/assessment-4

Fernandes, M.S., Brites, G.J.V.N., Costa, J.J., Gaspar, A.R., Costa, V.A.F., 2014. Review and future trends of solar adsorption refrigeration systems. Renew. Sustain. Energy Rev. https://doi.org/10.1016/j.rser.2014.07.081

Frazzica, A., Füldner, G., Sapienza, A., Freni, A., Schnabel, L., 2014. Experimental and theoretical analysis of the kinetic performance of an adsorbent coating composition for use in adsorption chillers and heat pumps. Appl. Therm. Eng. 73, 1020–1029. https://doi.org/10.1016/j.applthermaleng.2014.09.004

Frazzica, A., Palomba, V., Dawoud, B., Gullì, G., Brancato, V., Sapienza, A., Vasta, S., Freni, A., Costa, F., Restuccia, G., 2016. Design, realization and testing of an adsorption refrigerator based on activated carbon/ethanol working pair. Appl. Energy 174, 15–24. https://doi.org/10.1016/j.apenergy.2016.04.080

Hassan, H.Z., Mohamad, A.A., Alyousef, Y., Al-Ansary, H.A., 2015. A review on the equations of state for the working pairs used in adsorption cooling systems. Renew. Sustain. Energy Rev. 45, 600–609. https://doi.org/10.1016/j.rser.2015.02.008

International Energy Agency (IEA), 2019. Electricity Information: Overview. Stat. iea.

Kaushik, S.C., Reddy, V.S., Tyagi, S.K., 2011. Energy and exergy analyses of thermal power plants: A review. Renew. Sustain. Energy Rev. https://doi.org/10.1016/j.rser.2010.12.007

Mohammed, R.H., Askalany, A.A., 2019. Productivity Improvements of Adsorption Desalination Systems, in: Kumar, A., Prakash, O. (Eds.), Solar Desalination Technology. Springer Singapore, Singapore, pp. 325–357. https://doi.org/10.1007/978-981-13-6887-5_15

Mohammed, R.H., Mesalhy, O., Elsayed, M.L., Chow, L.C., 2019. Performance enhancement of adsorption beds with silica-gel particles packed in aluminum foams. Int. J. Refrig. https://doi.org/10.1016/j.ijrefrig.2019.03.013

Mohammed, R.H., Mesalhy, O., Elsayed, M.L., Chow, L.C., 2018. Scaling analysis of heat and mass transfer processes in an adsorption packed bed. Int. J. Therm. Sci. https://doi.org/10.1016/j.ijthermalsci.2018.07.017

Mohammed, R.H., Mesalhy, O., Elsayed, M.L., Chow, L.C., 2017. Novel compact bed design for

adsorption cooling systems: Parametric numerical study. Int. J. Refrig. https://doi.org/10.1016/j.ijrefrig.2017.04.028

Palomba, V., Vasta, S., Freni, A., Pan, Q., Wang, R., Zhai, X., 2017. Increasing the share of renewables through adsorption solar cooling: A validated case study. Renew. Energy. https://doi.org/10.1016/j.renene.2016.12.016

Pan, Q., Peng, J., Wang, H., Sun, H., Wang, R., 2019. Experimental investigation of an adsorption air-conditioner using silica gel- water working pair. Sol. Energy 185, 64–71. https://doi.org/10.1016/j.solener.2019.04.054

Restuccia, G., Freni, A., Maggio, G., 2002. A zeolite-coated bed for air conditioning adsorption systems: Parametric study of heat and mass transfer by dynamic simulation, in: Applied Thermal Engineering. pp. 619–630. https://doi.org/10.1016/S1359-4311(01)00114-4

Rouf, R.A., Jahan, N., Alam, K.C.A., Sultan, A.A., Saha, B.B., Saha, S.C., 2020. Improved cooling capacity of a solar heat driven adsorption chiller. Case Stud. Therm. Eng. 17, 100568.

Shmroukh, A.N., Ali, A.H.H., Ookawara, S., 2015. Adsorption working pairs for adsorption cooling chillers: A review based on adsorption capacity and environmental impact. Renew. Sustain. Energy Rev. 50, 445–456. https://doi.org/10.1016/j.rser.2015.05.035

Sircar, S., 1983. Linear-driving-force model for non-isothermal gas adsorption kinetics. J. Chem. Soc. Faraday Trans. 1 Phys. Chem. Condens. Phases 79, 785. https://doi.org/10.1039/f19837900785

Vasta, S., Brancato, V., La Rosa, D., Palomba, V., Restuccia, G., Sapienza, A., Frazzica, A., 2018. Adsorption Heat Storage: State-of-the-Art and Future Perspectives. Nanomaterials. https://doi.org/10.3390/nano8070522

Vodianitskaia, P.J., Soares, J.J., Melo, H., Gurgel, J.M., 2017. Experimental chiller with silica gel: Adsorption kinetics analysis and performance evaluation. Energy Convers. Manag. 132, 172–179. https://doi.org/10.1016/j.enconman.2016.11.028

Wang, D.C., Li, Y.H., Li, D., Xia, Y.Z., Zhang, J.P., 2010. A review on adsorption refrigeration technology and adsorption deterioration in physical adsorption systems. Renew. Sustain. Energy Rev. 14, 344–353. https://doi.org/10.1016/j.rser.2009.08.001

Wilkes, J.O., Birmingham, S.G., 2006. Fluid Mechanics for Chemical Engineers with Microfluidics and CFD. Pearson Education.

Younes, M.M., El-Sharkawy, I.I., Kabeel, A.E., Saha, B.B., 2017. A review on adsorbent-adsorbate pairs for cooling applications. Appl. Therm. Eng. 114, 394–414. https://doi.org/10.1016/j.applthermaleng.2016.11.138

Younes, M.M., El-sharkawy, I.I., Kabeel, A.E., Uddin, K., Pal, A., Mitra, S., Thu, K., Saha, B.B., 2019. Synthesis and characterization of silica gel composite with polymer binders for adsorption cooling applications. Int. J. Refrig. https://doi.org/10.1016/j.ijrefrig.2018.09.003

Zhang, L.Z., Wang, L., 1999. Effects of coupled heat and mass transfers in adsorbent on the

performance of a waste heat adsorption cooling unit. Appl. Therm. Eng. 19, 195–215. https://doi.org/10.1016/S1359-4311(98)00023-4